Journal of Computational and Applied Mathematics 394 (2021) 113538

Contents lists available at ScienceDirect

Journal of Computational and Applied Mathematics

journal homepage: www.elsevier.com/locate/cam

A stabilizer free weak Galerkin finite element method on polytopal mesh: Part III

Xiu Ye [a,1], Shangyou Zhang [b,*]

[a] Department of Mathematics, University of Arkansas at Little Rock, Little Rock, AR 72204, USA
[b] Department of Mathematical Sciences, University of Delaware, Newark, DE 19716, USA

ARTICLE INFO

Article history:
Received 21 February 2021

MSC:
primary 65N15
65N30
secondary 35J50

Keywords:
Weak Galerkin finite element methods
Second-order elliptic problems
Polytopal meshes
Superconvergence

ABSTRACT

A weak Galerkin (WG) finite element method without stabilizers was introduced in Ye and Zhang (2020) on polytopal mesh. Then it was improved in Ye and Zhang (2021) with order one superconvergence. The goal of this paper is to develop a new stabilizer free WG method on polytopal mesh. This method has convergence rates two orders higher than the optimal convergence rates for the corresponding WG solution in both an energy norm and the L^2 norm. The numerical examples are tested for low and high order elements in two and three dimensional spaces.

1. Introduction

A weak Galerkin finite element method without stabilizers on polytopal mesh has been developed in [1] and improved in [2] for the Poisson equation:

$$-\Delta u = f \quad \text{in } \Omega, \tag{1.1}$$

$$u = 0 \quad \text{on } \partial\Omega. \tag{1.2}$$

Here Ω is a polygonal or polyhedral domain. A stabilizing term is often needed in finite element methods with discontinuous approximations to ensure weak continuity of discontinuous functions across element boundaries. Development of stabilizer free discontinuous finite element method is desirable because it simplifies finite element formulation and reduces complexity of coding. However it is a difficult task on polygonal or polyhedral mesh.

The idea of removing stabilizers for the WG methods in [1,2] is how to approximate weak gradient ∇_w. A polynomial of degree j is used in [1,3] to approximate weak gradient ∇_w. Here $j = k+n-1$ and n is the number of sides of polytopal element. The authors in [4,5] have relaxed the requirement of polynomial degree of approximation. Rational function Wachspress coordinates [6] are used in [7,8] to approximate weak gradient. A new stabilizer free WG method has been introduced recently in [2] on polytopal mesh, which has order one superconvergence. Piecewise low order polynomials on a polytopal element are employed for ∇_w in [2], instead of using one piece high order polynomials in [1].

The goal of this paper is to introduce a new WG method without stabilizers on polygonal/polyhedral mesh, which has order two superconvergence, compared with order one superconvergence of the WG method in [2]. The superconvergence

* Corresponding author.
E-mail addresses: xxye@ualr.edu (X. Ye), szhang@udel.edu (S. Zhang).

1 Xiu Ye was supported in part by National Science Foundation, USA Grant DMS-1620016.

https://doi.org/10.1016/j.cam.2021.113538
0377-0427/

is proved for the numerical approximation in both an energy norm and the L^2 norm. Many numerical tests are conducted for the new WG elements of different degrees in two and three dimensional spaces.

2. Weak Galerkin finite element method

Let $\mathcal{T}_h$ be a partition of the domain Ω consisting of polygons/polyhedra that satisfies a set of conditions defined in [9]. Let $\mathcal{E}_h$ denote the set of all edges or flat faces in $\mathcal{T}_h$, and $\mathcal{E}_h^0 = \mathcal{E}_h \backslash \partial\Omega$ denote the set of all interior edges or flat faces. Denote by h_T the diameter of $T \in \mathcal{T}_h$ and mesh size $h = \max_{T\in\mathcal{T}_h} h_T$ for $\mathcal{T}_h$. Let $P_k(T)$ consist all the polynomials on T with degree less than or equal to k.

We define V_h the weak Galerkin finite element space for a given integer $k \geq 0$ as follows

$$V_h = \{v = \{v_0, v_b\} : \ v_0|_T \in P_k(T), \ v_b|_e \in P_{k+1}(e), \ e \subset \partial T, \ T \in \mathcal{T}_h\}. \tag{2.1}$$

Define V_h^0 a subspace of V_h as

$$V_h^0 = \{v : \ v \in V_h, \ v_b = 0 \text{ on } \partial\Omega\}. \tag{2.2}$$

A weak gradient $\nabla_w v$ for $v = \{v_0, v_b\} \in V_h$ is defined as a piecewise polynomial such that $\nabla_w v|_T \in \Lambda_k(T)$ for $T \in \mathcal{T}_h$ and

$$(\nabla_w v, \mathbf{q})_T = -(v_0, \nabla\cdot\mathbf{q})_T + \langle v_b, \mathbf{q}\cdot\mathbf{n}\rangle_{\partial T} \qquad \forall \mathbf{q} \in \Lambda_k(T). \tag{2.3}$$

We will define $\Lambda_k(T)$ in the next section.

Algorithm 1. A numerical approximation for (1.1)–(1.2) is seeking $u_h = \{u_0, u_b\} \in V_h^0$ that satisfies the following equation:

$$(\nabla_w u_h, \nabla_w v) = (f, \ v_0) \quad \forall v = \{v_0, v_b\} \in V_h^0. \tag{2.4}$$

The following notations will be adopted,

$$\begin{aligned}(v, w)_{\mathcal{T}_h} &= \sum_{T\in\mathcal{T}_h} (v, w)_T = \sum_{T\in\mathcal{T}_h} \int_T vw d\mathbf{x},\\ \langle v, w\rangle_{\partial\mathcal{T}_h} &= \sum_{T\in\mathcal{T}_h} \langle v, w\rangle_{\partial T} = \sum_{T\in\mathcal{T}_h} \int_{\partial T} vw ds.\end{aligned}$$

3. Existence and uniqueness

In this section, we will investigate the well posedness of the WG method. The space $H(div; \Omega)$ is defined as

$$H(div; \Omega) = \left\{\mathbf{v} \in [L^2(\Omega)]^d : \ \nabla\cdot\mathbf{v} \in L^2(\Omega)\right\}.$$

For any $T \in \mathcal{T}_h$, it can be divided into a set of disjoint triangles/tetrahedrons T_i with $T = \cup T_i$. Then we define $\Lambda_h(T)$ for the approximation of weak gradient on element T as

$$\begin{aligned}\Lambda_k(T) = \{\mathbf{v} \in H(div, T) : \ &\mathbf{v}|_{T_i} \in [P_{k+1}(T_i)]^d, \quad \nabla\cdot\mathbf{v} \in P_k(T).\\ &\mathbf{v}\cdot\mathbf{n}|_e \in P_{k+1}(e), \ e \subset \partial T\},\end{aligned} \tag{3.1}$$

Theorem 3.1. *For $\tau \in H(div, \Omega)$, there exists a projection Π_h with $\Pi_h\tau \in H(div, \Omega)$ satisfying $\Pi_h\tau|_T \in \Lambda_k(T)$ and*

$$(\nabla\cdot\tau, \ v_0)_T = (\nabla\cdot\Pi_h\tau, \ v_0)_T, \tag{3.2}$$

$$-(\nabla\cdot\tau, \ v_0)_{\mathcal{T}_h} = (\Pi_h\tau, \ \nabla_w v)_{\mathcal{T}_h}, \tag{3.3}$$

$$\|\Pi_h\tau - \tau\| \leq Ch^{k+2}|\tau|_{k+2}. \tag{3.4}$$

We will prove this important theorem in Section 5.

Let Q_0 be the element-wise defined L^2 projection onto $P_k(T)$ on each $T \in \mathcal{T}_h$. Similarly let Q_b be the L^2 projection onto $P_{k+1}(e)$ with $e \subset \partial T$. Let $\mathbb{Q}_h$ be the element-wise defined L^2 projection onto $\Lambda_k(T)$ on each element T. Finally we define $Q_h u = \{Q_0 u, Q_b u\} \in V_h$.

Lemma 3.1. *Let $\phi \in H^1(\Omega)$ and $v \in V_h^0$, then we have,*

$$\nabla_w Q_h\phi = \mathbb{Q}_h\nabla\phi. \tag{3.5}$$

Proof. It follows from (2.3), the definition of $\Lambda_k(T)$ and integration by parts that for any $\mathbf{q} \in \Lambda_k(T)$

$$\begin{aligned}(\nabla_w Q_h\phi, \mathbf{q})_T &= -(Q_0\phi, \nabla\cdot\mathbf{q})_T + \langle Q_b\phi, \mathbf{q}\cdot\mathbf{n}\rangle_{\partial T}\\ &= -(\phi, \nabla\cdot\mathbf{q})_T + \langle \phi, \mathbf{q}\cdot\mathbf{n}\rangle_{\partial T}\\ &= (\nabla\phi, \mathbf{q})_T\\ &= (\mathbb{Q}_h\nabla\phi, \mathbf{q})_T.\end{aligned}$$

Thus we have proved the identity (3.5). □

We define a semi-norm $|||\cdot|||$ for any $v \in V_h$ as

$$|||v|||^2 = (\nabla_w v, \nabla_w v)_{\mathcal{T}_h}. \tag{3.6}$$

We define another semi-norm as

$$\|v\|_{1,h} = \left(\sum_{T\in\mathcal{T}_h}\left(\|\nabla v_0\|_T^2 + h_T^{-1}\|v_0 - v_b\|_{\partial T}^2\right)\right)^{\frac{1}{2}}. \tag{3.7}$$

Obviously, $\|v\|_{1,h}$ define a norm for $v \in V_h^0$. We prove the equivalence of $|||\cdot|||$ and $\|\cdot\|_{1,h}$ in the following lemma.

Lemma 3.2. *There exist two positive constants C_1 and C_2 so that the following inequalities hold true for any $v = \{v_0, v_b\} \in V_h$,*

$$C_1\|v\|_{1,h} \le |||v||| \le C_2\|v\|_{1,h}. \tag{3.8}$$

Lemma 3.3. *The weak Galerkin finite element scheme (2.4) has a unique solution.*

The proofs for Lemmas 3.2 and 3.3 are similar to the ones in [2].

4. Error estimates

In this section, we will derive superconvergence for the WG finite element approximation u_h in both an energy norm and the L^2 norm.

4.1. Error estimates in energy norm

We start this subsection by deriving an error equation that $\epsilon_h = Q_h u - u_h$ satisfies. First we define

$$\ell(u, v) = (\mathbb{Q}_h\nabla u - \Pi_h\nabla u, \nabla_w v)_{\mathcal{T}_h}. \tag{4.1}$$

Lemma 4.1. *Let $\ell(u, v)$ defined in (4.1). Then we have*

$$(\nabla_w\epsilon_h, \nabla_w v) = \ell(u, v) \quad \forall v \in V_h^0. \tag{4.2}$$

Proof. For $v = \{v_0, v_b\} \in V_h^0$, testing (1.1) by v_0 and using (3.3), we have

$$(f, v_0) = -(\nabla\cdot\nabla u, v_0) = (\Pi_h\nabla u, \nabla_w v)_{\mathcal{T}_h}. \tag{4.3}$$

It follows from (3.5) and (4.3)

$$(\nabla_w Q_h u, \nabla_w v) = (f, v_0) + \ell(u, v). \tag{4.4}$$

Subtracting (2.4) from (4.4) gives the error equation,

$$(\nabla_w\epsilon_h, \nabla_w v) = \ell(u, v) \quad \forall v \in V_h^0.$$

This completes the proof of the lemma. □

For any function $\varphi \in H^1(T)$, the following trace inequality holds true (see [9] for details):

$$\|\varphi\|_e^2 \le C\left(h_T^{-1}\|\varphi\|_T^2 + h_T\|\nabla\varphi\|_T^2\right). \tag{4.5}$$

Theorem 4.1. *Let $u_h \in V_h$ and $u \in H^{k+3}(\Omega)$ be the solutions of (2.4) and (1.1), respectively. Then we have*

$$|||Q_h u - u_h||| \le Ch^{k+2}|u|_{k+3}. \tag{4.6}$$

Proof. Letting $v = \epsilon_h$ in (4.2), we arrive at

$$|||\epsilon_h|||^2 = \ell(u, \epsilon_h). \tag{4.7}$$

The definitions of $\mathbb{Q}_h$ and Π_h yield

$$\begin{aligned} |\ell(u, \epsilon_h)| &= |(\mathbb{Q}_h \nabla u - \Pi_h \nabla u, \nabla_w \epsilon_h)_{\mathcal{T}_h}| \\ &\le (\sum_T \|\mathbb{Q}_h \nabla u - \Pi_h \nabla u\|_T)^{1/2} |||\epsilon_h||| \\ &\le (\sum_T \|\mathbb{Q}_h \nabla u - \nabla u + \nabla u - \Pi_h \nabla u\|_T)^{1/2} |||\epsilon_h||| \\ &\le Ch^{k+2} |u|_{k+3} |||\epsilon_h|||. \end{aligned} \tag{4.8}$$

It follows (4.7) and (4.8),

$$|||\epsilon_h||| \le Ch^{k+2} |u|_{k+3}.$$

The proof of the theorem is completed. □

4.2. Error estimates in L^2 norm

First notice $\epsilon_h = \{\epsilon_0, \epsilon_b\} = Q_h u - u_h$. We use standard duality argument to derive L^2 error estimate. The dual problem is finding $\phi \in H_0^1(\Omega)$ such that

$$-\Delta \phi = \epsilon_0 \quad \text{in } \Omega, \tag{4.9}$$

and the following H^2 regularity holds

$$\|\phi\|_2 \le C \|\epsilon_0\|. \tag{4.10}$$

Lemma 4.2. *The following equation holds true for any $v \in V_h^0$,*

$$(\nabla_w Q_h \phi, \nabla_w v)_{\mathcal{T}_h} = (\epsilon_0, v_0) + \ell_1(\phi, v), \tag{4.11}$$

where

$$\ell_1(\phi, v) = \langle (\nabla \phi - \mathbb{Q}_h \nabla \phi) \cdot \mathbf{n}, v_0 - v_b \rangle_{\partial \mathcal{T}_h}.$$

Proof. For $v = \{v_0, v_b\} \in V_h^0$, testing (4.9) by v_0 gives

$$-(\Delta \phi, v_0) = (\epsilon_0, v_0). \tag{4.12}$$

Using integration by parts and the fact that $\sum_{T \in \mathcal{T}_h} \langle \nabla \phi \cdot \mathbf{n}, v_b \rangle_{\partial T} = 0$, we arrive at

$$-(\Delta \phi, v_0) = (\nabla \phi, \nabla v_0)_{\mathcal{T}_h} - \langle \nabla \phi \cdot \mathbf{n}, v_0 - v_b \rangle_{\partial \mathcal{T}_h}. \tag{4.13}$$

It follows from integration by parts, (2.3) and (3.5) that

$$\begin{aligned} (\nabla \phi, \nabla v_0)_{\mathcal{T}_h} &= (\mathbb{Q}_h \nabla \phi, \nabla v_0)_{\mathcal{T}_h} \\ &= -(v_0, \nabla \cdot (\mathbb{Q}_h \nabla \phi))_{\mathcal{T}_h} + \langle v_0, \mathbb{Q}_h \nabla \phi \cdot \mathbf{n} \rangle_{\partial \mathcal{T}_h} \\ &= (\mathbb{Q}_h \nabla \phi, \nabla_w v)_{\mathcal{T}_h} + \langle v_0 - v_b, \mathbb{Q}_h \nabla \phi \cdot \mathbf{n} \rangle_{\partial \mathcal{T}_h} \\ &= (\nabla_w Q_h \phi, \nabla_w v)_{\mathcal{T}_h} + \langle v_0 - v_b, \mathbb{Q}_h \nabla \phi \cdot \mathbf{n} \rangle_{\partial \mathcal{T}_h}. \end{aligned} \tag{4.14}$$

Combining (4.13) and (4.14) gives

$$-(\Delta \phi, v_0) = (\nabla_w Q_h \phi, \nabla_w v)_{\mathcal{T}_h} - \ell_1(\phi, v). \tag{4.15}$$

Combining (4.15) and (4.12) yields

$$(\nabla_w Q_h \phi, \nabla_w v)_{\mathcal{T}_h} = (\epsilon_0, v_0) + \ell_1(\phi, v). \tag{4.16}$$

This completes the proof of the lemma. □

By the same argument as (4.15), (4.2) has another form as

$$(\nabla_w \epsilon_h, \ \nabla_w v)_{\mathcal{T}_h} = \ell_1(u, v). \tag{4.17}$$

Theorem 4.2. *Let $u_h \in V_h$ be the weak Galerkin finite element solution of (2.4). Assume that the exact solution $u \in H^{k+3}(\Omega)$ and (4.10) holds true. Then, there exists a constant C such that for $k \geq 1$*

$$\|Q_0 u - u_0\| \leq Ch^{k+3}|u|_{k+3}. \tag{4.18}$$

Proof. Letting $v = \epsilon_h$ in (4.11) gives

$$\|\epsilon_0\|^2 = (\nabla_w Q_h\phi, \nabla_w \epsilon_h)_{\mathcal{T}_h} - \ell_1(\phi, \epsilon_h). \tag{4.19}$$

Letting $v = Q_h\phi$ in (4.17) gives

$$(\nabla_w \epsilon_h,\ \nabla_w Q_h\phi)_{\mathcal{T}_h} = \ell_1(u, Q_h\phi). \tag{4.20}$$

It follows from (4.19) and (4.20)

$$\|\epsilon_0\|^2 = \ell_1(u, Q_h\phi) - \ell_1(\phi, \epsilon_h). \tag{4.21}$$

By the Cauchy–Schwarz inequality, the trace inequality (4.5) and the definitions of $\mathbb{Q}_h$ and Q_h, then

$$\begin{aligned}
|\ell_1(u, Q_h\phi)| &\leq \left|\langle(\nabla u - \mathbb{Q}_h\nabla u)\cdot\mathbf{n},\ Q_0\phi - Q_b\phi\rangle_{\partial\mathcal{T}_h}\right| \\
&\leq C\left(\sum_{T\in\mathcal{T}_h} h_T\|\nabla u - \mathbb{Q}_h\nabla u\|_{\partial T}^2\right)^{1/2}\left(\sum_{T\in\mathcal{T}_h} h_T^{-1}\|Q_0\phi - \phi\|_{\partial T}^2\right)^{1/2} \\
&\leq Ch^{k+3}|u|_{k+3}|\phi|_2.
\end{aligned}$$

It follows from (4.5), (3.8) and (4.6)

$$\begin{aligned}
|\ell_1(\phi, \epsilon_h)| &= \left|\sum_{T\in\mathcal{T}_h}\langle(\nabla\phi - \mathbb{Q}_h\nabla\phi)\cdot\mathbf{n}, \epsilon_0 - \epsilon_b\rangle_{\partial T}\right| \\
&\leq C\left(\sum_{T\in\mathcal{T}_h} h_T\|\nabla\phi - \mathbb{Q}_h\nabla\phi\|_{\partial T}^2\right)^{\frac{1}{2}}\left(\sum_{T\in\mathcal{T}_h} h_T^{-1}\|\epsilon_0 - \epsilon_b\|_{\partial T}^2\right)^{\frac{1}{2}} \\
&\leq Ch^{k+3}|u|_{k+3}|\phi|_2.
\end{aligned}$$

Using the two estimates above, (4.21) becomes

$$\|\epsilon_0\|^2 \leq Ch^{k+3}|u|_{k+3}\|\phi\|_2.$$

Combining the above inequality with the regularity assumption (4.10), we obtain

$$\|\epsilon_0\| \leq Ch^{k+3}|u|_{k+3},$$

which completes the proof. □

5. Proof of Theorem 3.1

Theorem 3.1 is a corollary of the following lemma.

Lemma 5.1. *Let $\Pi_h : H(\mathrm{div}, \Omega) \to H(\mathrm{div}, \Omega) \cap \otimes\Lambda_{k-1}(T)$ be defined in (5.7). For $\mathbf{v} \in H(\mathrm{div}, \Omega)$ and for all $T \in \mathcal{T}_h$, we have,*

$$\begin{aligned}
(\Pi_h\mathbf{v},\ \mathbf{w})_T &= (\mathbf{v},\ \mathbf{w})_T \quad \forall\mathbf{w} \in [P_{k-2}(T)]^d, &(5.1)\\
\langle\Pi_h\mathbf{v}\cdot\mathbf{n},\ q\rangle_e &= \langle\mathbf{v}\cdot\mathbf{n},\ q\rangle_e \quad \forall q \in P_k(e), e \subset \partial T, &(5.2)\\
(\nabla\cdot\mathbf{v},\ q)_T &= (\nabla\cdot\Pi_h\mathbf{v},\ q)_T \quad \forall q \in P_{k-1}(T), &(5.3)\\
-(\nabla\cdot\mathbf{v},\ v_0)_{\mathcal{T}_h} &= (\Pi_h\mathbf{v},\ \nabla_w v)_{\mathcal{T}_h} \quad \forall v = \{v_0, v_b\} \in V_h^0, &(5.4)\\
\|\Pi_h\mathbf{v} - \mathbf{v}\| &\leq Ch^{k+1}|\mathbf{v}|_{k+1}. &(5.5)
\end{aligned}$$

Proof. We prove the lemma in 3D. The proof for 2D lemma is similar and much simpler.

We assume no additional inner edges is introduced when subdividing a polyhedron T into n tetrahedrons $\{T_i\}$. That is, we have precisely $n-1$ internal triangles which separate T into n parts. For simple notation, only one outside polygonal face e_1 of T is subdivided into m triangles, $e_{1,1}, \ldots, e_{1,m}$. For hexahedral finite elements [10–12], a face quadrilateral can be curved, i.e., the image of a square under a tri-linear mapping. Such a curved face polygon is taken as two face triangles of a polyhedron T.

On n tetrahedrons, a function of Λ_k can be expressed as

$$\mathbf{v}_h|_{T_{i_0}} = \sum_{i+j+l\le k} \begin{pmatrix} a_{1,ijl} \\ a_{2,ijl} \\ a_{3,ijl} \end{pmatrix} x^i y^j z^l, \ \ i_0 = 1, \dots, n. \tag{5.6}$$

$\mathbf{v}_h|_T$ is determined by $n \dim [P_k]^3 = n(k+1)(k+2)(k+3)/2$ coefficients. For any $\mathbf{v} \in H(\mathrm{div}; T)$, $\Pi_h \mathbf{v} \in \Lambda_k(T)$ is defined by

$$\int_{e_{ij}\subset\partial T} (\Pi_h\mathbf{v} - \mathbf{v})\cdot\mathbf{n}_{ij} p_k dS = 0 \qquad \forall p_k \in P_k(e_{ij}),\, e_{ij} \ne e_{1,\ell},\, \ell \ge 2, \tag{5.7a}$$

$$\int_{e_{11}\subset\partial T} (\Pi_h\mathbf{v}|_{e_{11}} - \Pi_h\mathbf{v}|_{e_{1j}})\cdot\mathbf{n}_{11} p_k dS = 0 \qquad \forall p_k \in P_k(e_{1j}), j = 2, \dots, m, \tag{5.7b}$$

$$\int_{e_{ij}\subset T^0} (\Pi_h\mathbf{v} - \mathbf{v})\cdot\mathbf{n}_{ij} p_k dS = 0 \qquad \forall p_k \in P_k(e_{ij}) \setminus P_0(e_{ij}), \tag{5.7c}$$

$$\int_{e_{ij}\subset T^0} [\Pi_h\mathbf{v}]\cdot\mathbf{n}_{ij} p_k dS = 0 \qquad \forall p_k \in P_k(e_{ij}), \tag{5.7d}$$

$$\int_T (\Pi_h\mathbf{v} - \mathbf{v})\cdot\nabla p_{k-1} d\mathbf{x} = 0 \qquad \forall p_{k-1} \in P_{k-1}(T) \setminus P_0(T), \tag{5.7e}$$

$$\int_{T_i} (\Pi_h\mathbf{v} - \mathbf{v})\cdot p d\mathbf{x} = 0 \qquad \forall p \in CP(T_i), \ \ i = 1, \dots, n, \tag{5.7f}$$

$$\int_{T_1} \nabla\cdot(\Pi_h\mathbf{v}|_{T_i} - \Pi_h\mathbf{v}|_{T_1}) p_{k-1} d\mathbf{x} = 0 \qquad \forall p_{k-1} \in P_{k-1}(T_1), \ \ i = 2, \dots, n, \tag{5.7g}$$

where e_{ij} is the jth face triangle of T_i with a fixed normal vector $\mathbf{n}_{ij}$, $[\cdot]$ denotes the jump on a face triangle, $\Pi_h\mathbf{v}|_{T_i}$ is understood as a polynomial vector which can be used on another tetrahedron T_1, $e_{1j} \subset e_1 \subset \partial T$ is a face triangle of T_{i_j}, $\Pi_h\mathbf{v}|_{e_{1j}}$ is extended to the whole e_1 as one polynomial, and curl-polynomial space

$$\begin{aligned} CP(T_i) = \{\mathbf{v} \in & [P_k(T_i)]^3 \ | \ \mathbf{v}\cdot\mathbf{n}_{ij} = 0 \text{ on } e_{ij} \subset \partial T_i, \\ & \int_{T_i} \mathbf{v}\cdot\nabla p_{k-1} d\mathbf{x} = 0 \quad \forall p_{k-1} \in P_{k-1}(T_i)\}, \end{aligned}$$

where e_{ij} also denotes the four face triangles of T_i. The linear system (5.7) of equations has the following number of equations,

$$\begin{aligned} & (2n+3-m)\frac{(k+1)(k+2)}{2} + (m-1)\frac{(k+1)(k+2)}{2} \\ & + (n-1)\frac{(k+1)(k+2)-2}{2} + (n-1)\frac{(k+1)(k+2)}{2} \\ & + \frac{k(k+1)(k+2)-6}{6} \\ & + n\Big(\frac{(k-1)k(k+1)}{2} - \frac{(k-2)(k-1)k}{6}\Big) \\ & + (n-1)\frac{k(k+1)(k+2)}{6} \\ = & \frac{n(k+1)(k+2)(k+3)}{2}, \end{aligned}$$

which is exactly the number of coefficients for a $\mathbf{v}_h$ function in (5.6). Thus we have a square linear system. The square system has a unique solution if and only if the homogeneous system has the trivial solution.

Let $\mathbf{v} = 0$ in (5.7). By (5.7a) and (5.7b), $\Pi_h\mathbf{v}\cdot\mathbf{n} = 0$ on the whole boundary ∂T. By (5.7c) and (5.7d), $\int_{e_{ij}} [\Pi_h\mathbf{v}\cdot\mathbf{n}_{ij}] dS = 0$ and $\int_{e_{ij}} \Pi_h\mathbf{v}\cdot\mathbf{n}_{ij} p dS = 0$ for all $p \in P_k \setminus P_0$ on inter-element triangles e_{ij}. By (5.7g), $\nabla\cdot\Pi_h\mathbf{v}$ is a one-piece polynomial on the whole T. Therefore, by (5.7e), we have

$$\begin{aligned} & \int_T (\nabla\cdot\Pi_h\mathbf{v})^2 d\mathbf{x} \\ = & \sum_{i=1}^n \Big(\int_{T_i} -\Pi_h\mathbf{v}\cdot\nabla(\nabla\cdot\Pi_h\mathbf{v}) d\mathbf{x} + \int_{\partial T_i} \Pi_h\mathbf{v}\cdot\mathbf{n}(\nabla\cdot\Pi_h\mathbf{v}) dS \Big) \\ = & \, 0. \end{aligned} \tag{5.8}$$

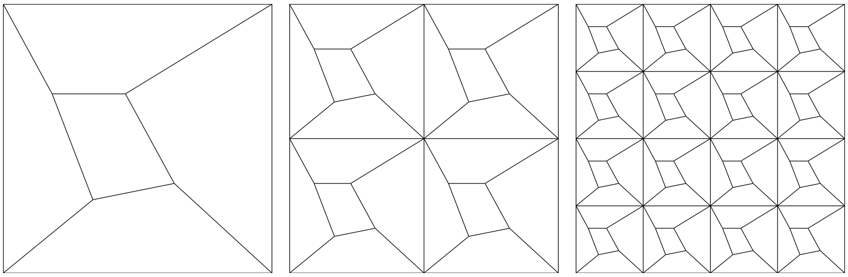

Fig. 6.1. The first three levels of quadrilateral grids, for Table 6.1.

That is,

$$\nabla \cdot \Pi_h \mathbf{v} = 0 \quad \text{on } T.$$

Thus

$$\Pi_h \mathbf{v}|_{T_i} \in CP(T_i), \quad i = 1, \ldots, n. \tag{5.9}$$

By (5.7f), $\Pi_h \mathbf{v} = \mathbf{0}$. Hence $\Pi_h \mathbf{v}$ is well defined.

For any $\mathbf{w} \in [P_{k-2}(T)]^3$, we have $\mathbf{w} = \nabla p_{k-1} + \nabla \times \mathbf{q}_{k-1}$ on all T_i, where $\mathbf{q}_{k-1}|_{T_i} \in [P_{k-1}(T_i)]^3$ can be chosen such that $\nabla \times \mathbf{q}_{k-1} \in CP(T_i)$. By (5.7e) and (5.7f), (5.1) holds.

(5.2) follows (5.7a) and (5.7b).

Replacing one $\nabla \cdot \Pi_h \mathbf{v}$ by q in (5.8), (5.3) follows.

It follows from (2.3) and (5.3) that for $v = \{v_0, v_b\} \in V_h^0$

$$\begin{aligned} -(\nabla \cdot \mathbf{v},\ v_0)_{\mathcal{T}_h} &= -(\nabla \cdot \Pi_h \mathbf{v},\ v_0)_{\mathcal{T}_h} \\ &= -(\nabla \cdot \Pi_h \mathbf{v},\ v_0)_{\mathcal{T}_h} + \langle v_b, \Pi_h \mathbf{v} \cdot \mathbf{n} \rangle_{\partial \mathcal{T}_h} \\ &= (\Pi_h \mathbf{v},\ \nabla_w v)_{\mathcal{T}_h}, \end{aligned}$$

which proves (5.4).

On a size-one T, by the finite dimensional norm-equivalence and the shape regularity assumption on sub-triangles, the interpolation is stable in $L^2(T)$, i.e.,

$$\|\Pi_h \mathbf{v}\|_T \le C \|\mathbf{v}\|_T. \tag{5.10}$$

After a scaling, the constant C in (5.10) remains same for all $h > 0$. Since $[P_k(T)]^3 \subset \Lambda_k$ and Π_h is uni-solvent, $\Pi_h \mathbf{v} = \mathbf{v}$ for all $\mathbf{v} \in [P_k(T)]^3$. It follows that, by Π_h's P_k-polynomial preservation,

$$\begin{aligned} \|\Pi_h \mathbf{v} - \mathbf{v}\|^2 &\le C \sum_{T \in \mathcal{T}_h} (\|\Pi_h(\mathbf{v} - p_{k,T})\|_T^2 + \|p_{k,T} - \mathbf{v}\|_T^2) \\ &\le C \sum_{T \in \mathcal{T}_h} (C\|\mathbf{v} - p_{k,T}\|_T^2 + \|p_{k,T} - \mathbf{v}\|_T^2) \\ &\le C \sum_{T \in \mathcal{T}_h} h^{2k+2} |\mathbf{v}|_{k+1,T}^2 \\ &= Ch^{2k+2} |\mathbf{v}|_{k+1}^2, \end{aligned}$$

where $p_{k,T}$ is the kth Taylor polynomial of $\mathbf{v}$ on T. $\square$

6. Numerical experiments

We solve the Poisson problem (1.1)–(1.2) on the unit square domain with the exact solution

$$u = \sin(\pi x) \sin(\pi y). \tag{6.1}$$

We compute the solution (6.1) on a type of quadrilateral grids, shown in Fig. 6.1. Here to avoid convergence to parallelograms under the nest refinement of quadrilaterals, we fix the shape of quadrilaterals on all levels of grids. We list the computation in Table 6.1. We have two orders of superconvergence in L^2-norm and in H^1-like norm for all order finite elements, except for P_0 element which has only one order superconvergence in L^2 norm. Both cases confirm the theoretic convergence rates.

Table 6.1
Error profiles and convergence rates on quadrilateral grids shown in Fig. 6.1 for (6.1).

Level	$\lVert Q_h u - u_h \rVert_0$	Rate	$\lVert\lVert Q_h u - u_h \rVert\rVert$	Rate
	By the P_0–$P_1(\Lambda_0)$ WG element			
6	0.2533E−03	2.00	0.1448E−02	2.00
7	0.6337E−04	2.00	0.3620E−03	2.00
8	0.1584E−04	2.00	0.9050E−04	2.00
	By the P_1–$P_2(\Lambda_1)$ WG element			
5	0.9360E−06	4.00	0.2156E−03	3.00
6	0.5851E−07	4.00	0.2696E−04	3.00
7	0.3663E−08	4.00	0.3371E−05	3.00
	By the P_2–$P_3(\Lambda_2)$ WG element			
4	0.7659E−06	4.98	0.1487E−03	3.99
5	0.2404E−07	4.99	0.9307E−05	4.00
6	0.7521E−09	5.00	0.5819E−06	4.00
	By the P_3–$P_4(\Lambda_3)$ WG element			
2	0.1439E−03	3.84	0.9642E−02	3.24
3	0.2319E−05	5.95	0.3065E−03	4.98
4	0.3646E−07	5.99	0.9620E−05	4.99

Table 6.2
Error profiles and convergence rates on polygonal grids shown in Fig. 6.2 for (6.1).

Level	$\lVert Q_h u - u_h \rVert_0$	Rate	$\lVert\lVert Q_h u - u_h \rVert\rVert$	Rate
	By the P_0–$P_1(\Lambda_0)$ WG element			
6	0.2524E−03	2.00	0.1313E−02	2.00
7	0.6315E−04	2.00	0.3282E−03	2.00
8	0.1579E−04	2.00	0.8204E−04	2.00
	By the P_1–$P_2(\Lambda_1)$ WG element			
6	0.4117E−07	4.00	0.1620E−04	3.00
7	0.2574E−08	4.00	0.2025E−05	3.00
8	0.1615E−09	3.99	0.2531E−06	3.00
	By the P_2–$P_3(\Lambda_2)$ WG element			
4	0.3371E−06	4.98	0.7750E−04	3.99
5	0.1058E−07	4.99	0.4849E−05	4.00
6	0.3417E−09	4.95	0.3032E−06	4.00
	By the P_3–$P_4(\Lambda_3)$ WG element			
2	0.5538E−04	4.17	0.4462E−02	3.32
3	0.8817E−06	5.97	0.1414E−03	4.98
4	0.1382E−07	6.00	0.4436E−05	4.99

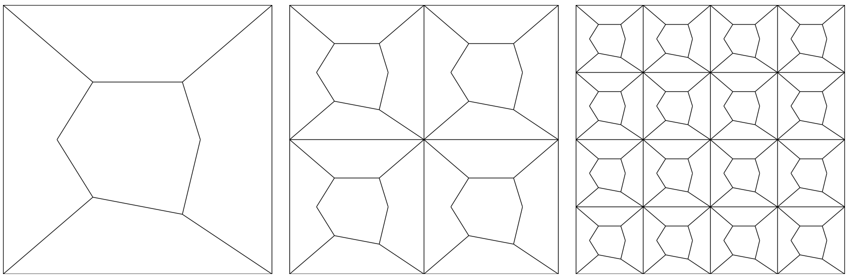

Fig. 6.2. The first three levels of quadrilateral-hexagon grids, for Table 6.2.

Next we solve the same problem (6.1) on a type of grid with quadrilaterals and hexagons, shown in Fig. 6.2. We list the result of computation in Table 6.2 where all theoretic convergence results are matched.

We solve 3D problems (1.1)–(1.2) on the unit cube domain $\Omega = (0, 1)^3$ with the exact solution

$$u = \sin(\pi x)\sin(\pi y)\sin(\pi z). \tag{6.2}$$

Here we use a uniform wedge-type (polyhedron with 2 triangular faces and 3 rectangular faces) grids, shown in Fig. 6.3. Here each wedge is subdivided into three tetrahedrons with three rectangular faces being cut each into two triangles,

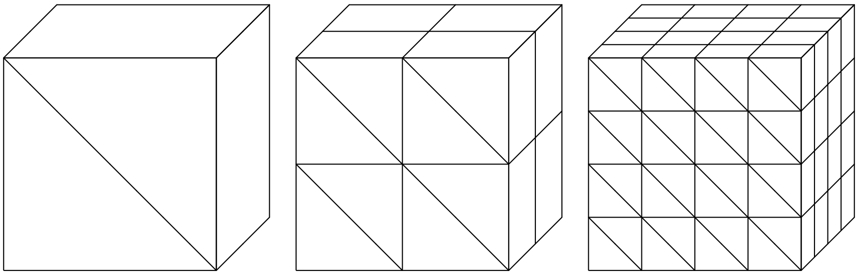

Fig. 6.3. The first three levels of wedge grids used in Table 6.3.

Table 6.3
Error profiles and convergence rates on grids shown in Fig. 6.3 for (6.2).

Level	$\|Q_h u - u_h\|_0$	Rate	$\|\|Q_h u - u_h\|\|$	Rate
	By the P_0–$P_1(\Lambda_0)$ WG element			
4	0.0101282	1.8	0.1286817	2.0
5	0.0026250	1.9	0.0324419	2.0
6	0.0006623	2.0	0.0081278	2.0
	By the P_1–$P_2(\Lambda_1)$ WG element			
4	0.0001608	3.9	0.0250022	3.0
5	0.0000102	4.0	0.0031359	3.0
6	0.0000006	4.0	0.0003923	3.0
	By the P_2–$P_3(\Lambda_0)$ WG element			
3	0.0003973	4.9	0.0701007	3.9
4	0.0000126	5.0	0.0044450	4.0
5	0.0000004	5.0	0.0002788	4.0
	By the P_3–$P_4(\Lambda_0)$ WG element			
3	0.7113E−04	5.9	0.1988E−01	4.9
4	0.1126E−05	6.0	0.6295E−03	5.0
5	0.1767E−07	6.0	0.1974E−04	5.0

when defining a piecewise polynomial space Λ_k for the weak gradient. The results are listed in Table 6.3, confirming the two-order superconvergence in the two norms for all polynomial-degree $k \geq 1$ elements.

References

[1] X. Ye, S. Zhang, A stabilizer-free weak Galerkin finite element method on polytopal meshes, J. Comput. Appl. Math. 371 (2020) 112699, arXiv:1906.06634.
[2] X. Ye, S. Zhang, A stabilizer free weak Galerkin finite element method on polytopal mesh: Part II, J. Comput. Appl. Math. 394 (2021) 113525, arXiv:2008.13631.
[3] X. Ye, S. Zhang, A conforming discontinuous Galerkin finite element method: Part II, Int. J. Numer. Anal. Model. 17 (2) (2020) 281–296.
[4] A. Al-Taweel, X. Wang, A note on the optimal degree of the weak gradient of the stabilizer free weak Galerkin finite element method, Appl. Numer. Math. 150 (2020) 444–451.
[5] A. Al-Taweel, X. Wang, The lowest-order stabilizer free weak Galerkin finite element method, Appl. Numer. Math. 157 (2020) 434–445.
[6] W. Chen, Y. Wang, Minimal degree $H(curl)$ and $H(div)$ conforming finite elements on polytopal meshes, Math. Comp. 86 (2017) 2053–2087.
[7] J. Liu, S. Tavener, Z. Wang, Lowest-order weak Galerkin finite element method for Darcy flow on convex polygonal meshes, SIAM J. Sci. Comput. 40 (2018) 1229–1252.
[8] L. Mu, Pressure robust weak Galerkin finite element methods for Stokes problems, SIAM J. Sci. Comput. 42 (2020) B608–B629.
[9] J. Wang, X. Ye, A weak Galerkin mixed finite element method for second-order elliptic problems, Math. Comp. 83 (2014) 2101–2126.
[10] S. Zhang, On the nested refinement of quadrilateral and hexahedral finite elements and the affine approximation, Numer. Math. 98 (3) (2004) 559–579.
[11] S. Zhang, Numerical integration with Taylor truncations for the quadrilateral and hexahedral finite elements, J. Comput. Appl. Math. 205 (1) (2007) 325–342.
[12] S. Zhang, S. Zhang, C0P2-P0 Stokes finite element pair on sub-hexahedron tetrahedral grids, Calcolo 54 (4) (2017) 1403–1417.